J. Ind. Geophys. Union, 30(1) (2026), 6-20
https://doi.org/10.71122/JIGU.30(1)2026.002

Crust-mantle seismic structure along Jakhau-Mandvi DSS Profile: A geodynamic perspective

K. Chandrakala* and Prakash Kumar
CSIR- National Geophysical Research Institute, Uppal Road ,
Hyderabad- 500 007, India
*corresponding Author: chndrbhat@gmail.com

ABSTRACT

Kutch rift basin situated in the northwestern part of the Deccan volcanic province, is characterised by sustained intermediate to deep crustal earthquake activity since historical times, unheard in other global stable terrains. This region underwent through several geotectonic, thermal and magmatic episodes in the past, whose signatures are manifested in various forms including the complex and heterogeneous crust-mantle velocity structure. In order to delineate hydrocarbon-rich Mesozoic sediments and underlying basement configuration, seismic refraction and wide-angle reflection data was acquired along the four Deep Seismic Sounding profiles. In the present study, we reprocessed the seismic data along one of these profiles, shot across the southwestern part of the Kutch region, that runs from Jakhau to Mandvi on the west coast. Our study delineated occurrence of a six-layered sequence above the granitic–gneissic basement (Vp: 5.90–6.00 km/s), with their thicknesses varying from 5.5 to 8 km. It includes, Tertiary sediments (Vp: 2.0 km/s), Deccan basalts (Vp: 4.70 km/s), upper low velocity Mesozoic sediments (Vp: 3.3 km/s), Mesozoic limestone (Vp : 5.1 km/s) followed by Mesozoic volcanics (Vp: 5.50 km/s) and another low velocity Mesozoic sediments (Vp: 5.30 km/s). It is underlain by mid-crustal layer (Vp: 6.30-6.40 km/s) located at depths of around 8 to 12.5 km, which is further underlain by a relatively thinner lower crustal layer (Vp: 6.80-6.90 km/s). Below this layer, we also delineated two distinct underplated magmatic layers (Vp: 7.20 -7.50 km/s) above the Moho, characterize by velocity 7.7-8.0 km/s. Moho is delineated at an extremely shallow depths from 25 to 35 km. Conspicuously, we also depicted a frozen mantle magma chamber (Vp: 8.0 km/s), in the uppermost mantle, which coincides with the location of Katrol Hill Fault. It appears that this region has undergone persistent magmatism, massive subcrustal erosion and asthenospheric upwarping.

Keywords: Kutch seismic zone, Mesozoic sediments, Deccan volcanic province, Magmatic underplating, Frozen mantle magma chamber, Crust-mantle seismic velocity structure, Geodynamics.

INTRODUCTION

Precambrian Indian shield has been associated with a number of rifting episodes, continental breakups and multiple plume interactions that have severely modified its crust-mantle structure on a large scale, (Pandey, 2020). It contains several rift valleys, mega shear zones and lineaments, which have remained active since at least Mesoproterozoic period (Rogers and Callahan, 1987). Consequent to such changes, it has been experiencing moderate-to-large intraplate seismic activity since historical times, which is unheard in other global stable regions. GPS and seismological studies have clearly revealed high strain rates over many parts of the Indian terrain (Talwani and Gangopadhyay, 2001; Paul et al., 2001), compared to much lower strain rates elsewhere in other stable continental regions (Johnston, 1994).

Kutch rift region, located in NW part of Indian subcontinent, is one such region, which is seismically quite active and where intermediate to deep crustal earthquakes of varying magnitudes, keep on occurring. Similar events have also been reported from other global rift zones, like Amazonian (Brazil), East African (Africa), Baikal (Russia), Rio Grande (North America), Narmada-Son (India) and Reelfoot (New-Madrid, USA) (Mukherjee, 1942; Mooney et al., 1983; Prodehl et al., 1994; Johnston, 1996; Liu and Zoback, 1997; Singh et al., 1999; Kruger et al., 2002; Wilson et al., 2003; Gao et al., 2004). Nevertheless, the Kutch region remains a unique site of sustained intraplate seismicity for a long time. Rajendran and Rajendran (2001) reported some 15 historical and recent earthquakes of magnitude 5 to 6 that took place in this region earlier. This was also substantiated by paleo-seismological studies, which confirmed such occurrences since 325 BC (Rajendran et al., 2008). In fact, during last couple of hundred years alone, it has witnessed three large earthquakes (besides numerous moderate events) like, 1819 Kachchh (Mw: 7.8), 1956 Anjar (Mw: 6.0) and 2001 Bhuj (Mw: 7.7), the last one causing widespread damage and killed more than 20,000 people (Chung and Gao, 1995; Gupta et al., 2001; Rajendran and Rajendran, 2001; Rajendran et al., 2008; Mandal and Pandey, 2010, 2011; Pandey, 2020).

Geotectonically, this region severely suffered through many tectonic, thermal and magmatic episodes including Deccan volcanism, scars of which are amply manifested in the form of complex and heterogeneous crust-mantle velocity structure, as revealed by seismological and other geological and geophysical studies (Biswas, 1987; Gambos et al., 1995; Kayal et al., 2002; Mandal, 2006, 2007; Mandal and Pujol, 2006; Mandal and Chadha, 2008; Mandal and Pandey, 2010, 2011). In order to delineate Mesozoic sediment thickness, basement configuration and shallow crustal seismic structure, seismic refraction and wide-angle reflections data was acquired along four DSS profiles, (i) Jakhau-Mandvi, (ii) Mandvi-Mundra, (iii) Mundra –Adesar, and (iv) Hamipur-Halvad, by CSIR-National Geophysical Research Institute, Hyderabad (India) during 1996-1997. These profiles trend NW-S, W-E, SW-NE and N-S directions respectively and cut across several geotectonic units of the region.

Prasad et al., (2010) provided basement structure along these profiles, while preliminary seismic-reflection images of the crust was given by Sarkar et al., (2007). Earthquake tomographic and seismic refraction studies have earlier also indicated presence of crustal intrusives and thick underplated magmatic layer at lower crustal levels, as well as below the Moho (Sarkar et al., 2007; Kayal et al., 2002; Mandal and Chadha, 2008; Mandal and Pandey, 2010, 2011). In the present study, we made an attempt to delineate the detailed shallow and deep crustal-upper most mantle seismic structure along the Jakhau-Mandvi profile, shot across the NW-SE segment of the Kutch basin (Figure 1). This study has provided a new light on the geodynamic evolution of the western Indian region.

REGIONAL GEOLOGY AND TECTONICS

The seismically active east–west trending intra-continental Kutch rift basin, is located between 22° 30' and 24° 30' N and 68° and 72° E in the Kutch district of Gujarat, India (Figure 1) (Biswas, 2005; Mandal and Pandey, 2010, 2011). This severely faulted basin, which is about 400 km in length and 150 km in width, has a typical geometry of an asymmetric rift basin, which is bounded by Nagar Parkar fault (NPF) in the north and the North Kathiwar Fault (NKF) in the south (Merh, 1995; Biswas, 2005). It is characterized by three main uplifted blocks (Island Belt, Kutch Mainland and Wagad) with intervening grabens and half-grabens. The Other major faults in the region are, the E–W trending Allah Bund fault, Island Belt Fault, Kutch Mainland Fault and Katrol Hill fault (KHF). A meridional/median high zone forms the another striking feature. This basin is slightly tilted towards the south and contains about 3–5 km thick young Tertiary and Mesozoic sediments that overly Precambrian basement (Biswas, 1987). It preserves the longest record of the Mesozoic succession in the western India, which are often folded, faulted, uplifted, and intruded by 66 Ma Deccan volcanics (Biswas, 1987, 2005). Besides, it is also characterised by a series of east–west trending uplifted structures, formed as a result of crustal movements of discrete basement blocks along the pre-existing ancient faults, which may have association with the concealed Delhi orogenic belt trends.

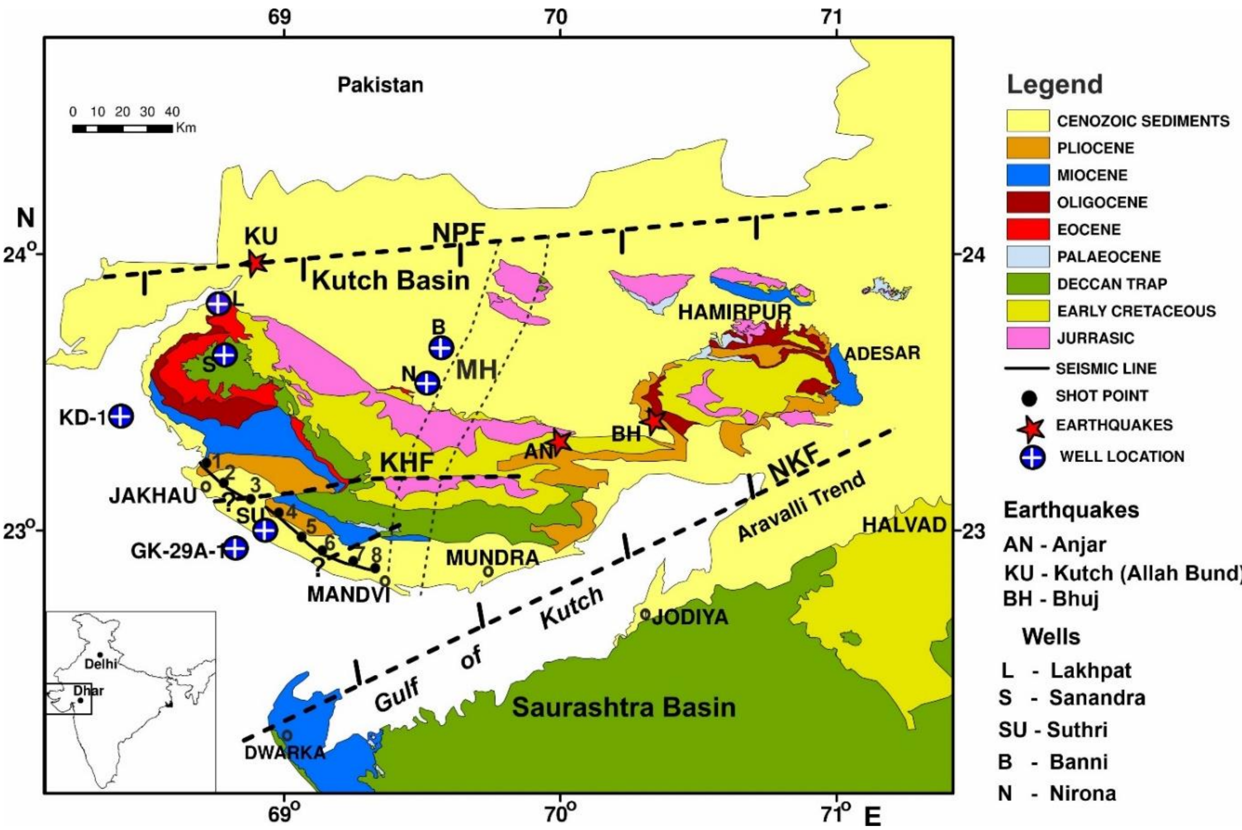

Figure 1. Geological and tectonic map of Kutch basin along with the location of the seismic refraction and wide-angle reflection profile. Solid blue circles encircling '+' represents well locations. L: Lakhpat; S: Sanandra; Su: Suthri; B: Banni; N: Nirona. Major earthquakes are shown with red stars and their names are represented by AN: Anjar Earthquake (1956); BH: Bhuj Earthquake (2001); KU : Kutch Earthquake (1819) (Allah bund Earthquake). Faults are shown with black dashed lines. NPF- Nagar Parkar Fault; NKF: North Kathiawar Fault; KHF-Katrol Hill Fault; MH: Median high. The black solid circles with numbers indicate Shot Points. NPF and NKF are considered the northern, southern boundaries of the Kutch rift basin.

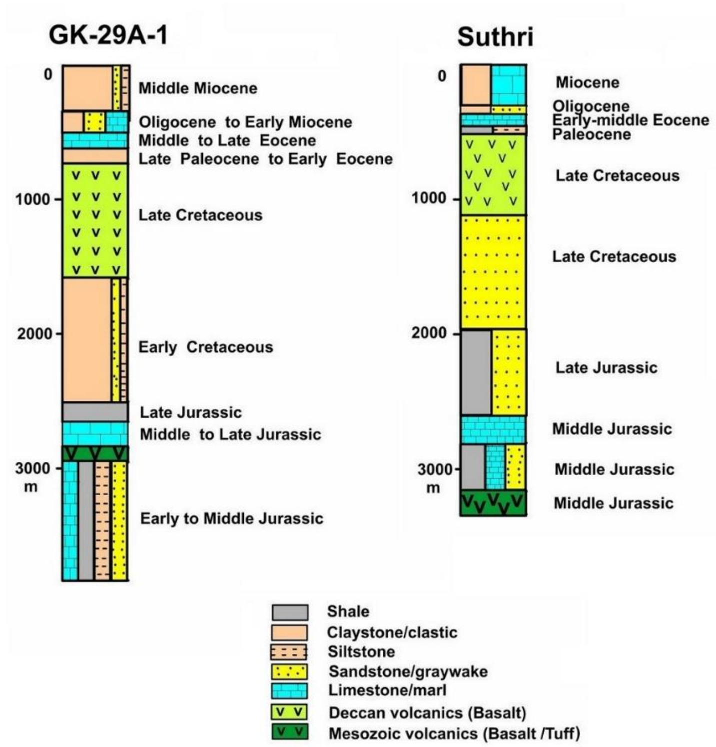

Figure 2. Lithostratigraphic sections encountered in the drilled deep wells, located over onshore and offshore regions. Their locations are shown in Figure 1 (Singh et al., 1997; DGH, 2015)

This basin is also severely affected by 66 Ma Deccan volcanism, as well as Jurassic magmatism, which occurred during Antarctica-Africa rifting phase related to the east Gondwana breakup period, as evidenced by their occurrences at subsurface depths in GK 29A-1, Suthri, Lakhapt and Lodhika drilled boreholes (DGH, 2015). The lithostratigraphy of the region, as pearced by GK 29A-1 and Suthri boreholes, are shown in Figure 2. Similarly, small patches of Deccan volcanics can be seen exposed close to its south-west periphery, west of Anjar. On its eastern side, it is separated from the Cambay rift while on its western side, it extends into offshore areas of the Arabian sea. Geodynamically, this region is also affected by the NE–SW compressive stress, consequent to collision of Indian and Eurasian plates. Being an ancient rift basin, it has been persistently active prior to and during the Deccan volcanic episode (Biswas, 1987) and India –Eurasia collision as well.

SEISMIC STUDIES

Data Acquisition

The seismic refraction / wide angle reflection data along Jakhau - Mandvi (NW-SE) profile was acquired by the Controlled Source Seismic (CSS) group of CSIR- National Geophysical Research Institute, using two 60 channel Texas Instrument model DFS-V recording systems (NGRI, 2000). Data was recorded with a spread length of 11.9 km and geophone spacing of about 100 m. Each spread was recorded with a number of shot points of varying offsets 10 to 50 km. Shot holes were drilled to a depth of 20 m, with 10 m of hole to hole distance in a rectangular / triangular pattern. Each shot is loaded on average with 50 kg high energy explosives (Open Case Gelignite 83 mm/Telgex LD 83 mm). To enhance the signal, four to six geophones of natural frequency 4.5 Hz were connected in series and bundled at each geophone position. A notch filter (with 50 Hz frequency) was kept in operation to minimize the effects of power line pick up. Data was recorded in both analog as well digital form up to 20 seconds. Due to logistic reasons, there was a gap in data acquisition, which was shown in the surface coverage map (Figure 3).

Data processing

The Jakhau – Mandvi profile consists of 8 shot points, with good quality recorded data, as is evident from the field seismograms of the shot points SP2 and SP7 (Figure 4 a, b). The signal-to-noise ratio of the first arrivals is good across most of the sections. Strong reflection phases are very clear at offset of 20 to 60 km from the shot location. From this figure, a travel time jump in the first arrival refraction times is clearly noticeable, which indicates that the refractions are not reaching to the surface for a particular time window, and this delay in time, appears as a skip on the seismograms. Such shift in first arrival travel times (skip) occur due to certain geological conditions.

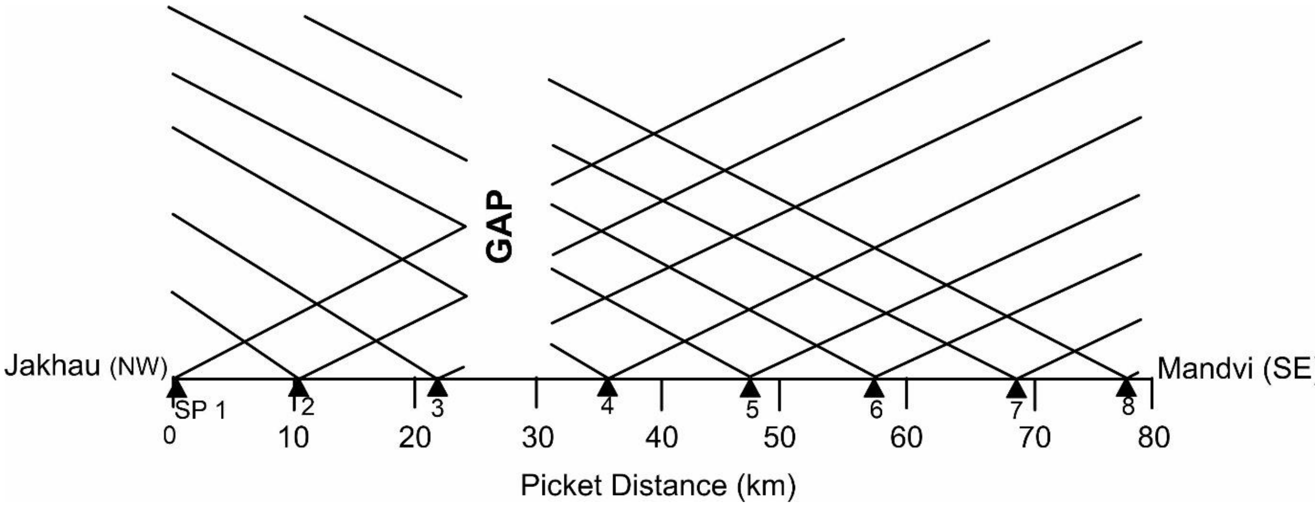

Figure 3. Schematic diagram of the surface coverage along the Jakhau-Mandvi seismic profile.

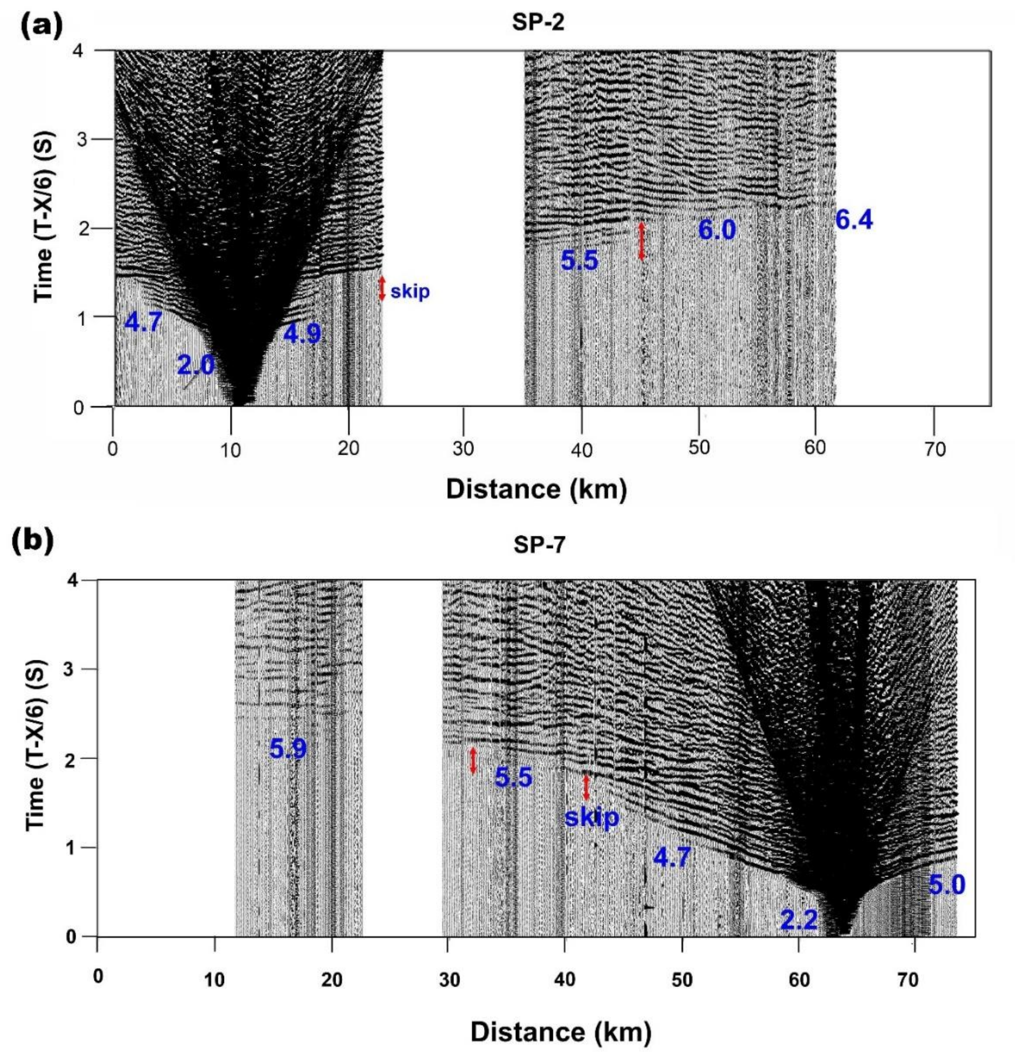

Figure 4. Shot gathers of shot points, **(a)** SP 2 and **(b)** SP 7, along the Jakhau – Mandvi seismic profile. Various phases and corresponding velocities are marked with number (km/s). Skip in the travel time is marked with red arrow (not to scale), which is ascribed to the presence of low velocity layer.

Theoretically, the necessary condition in seismic refraction method is that the velocities of all the underlying layers should increase with depth. In such cases, the first arrival refraction from each layer appear as a continuous segment, without any break. If there is a break or jump in the first arrivals, then it usually occurs in two cases: (i) if the velocity of a layer is lower than that of the overlying layer, no critically refracted waves will be generated from the top of the low-velocity layer (Dobrin, 1976) and this layer is not detected in the first-arrival time-distance plot (Whiteley and Greenhalgh, 1979; Lutter et al., 1994; Tewari et al., 1995; Dixit et al., 2000; Koteswara Rao et al., 2004, Kolluru and Behera, 2025) (ii) The other possibility of skip could be due to a fault. Importantly, we have noticed presence of skip in all the seismograms in every shot point data; SP 2 and SP 7 being shown in Figure 4. Thus, the skip occurrence due to a fault is not tenable, as a fault is a localized phenomena. Thus, based on the seismic data, the skip in the present study in considered due to presence of a low velocity only.

Similarly, to strengthen our assumption, we have looked in to the two drilled bore wells, one located near the present studied profile (Suthri around 10 km from SP4) and the other one, GK 29A-1 situated in the nearby onshore region (Figures 1 and 2). Based on the lithostratigraphy of the drilled bore wells (Figure 2), the Tertiary sediments is defined as layer-1; Deccan basalt, layer-2; sandstone, layer-3; limestone, layer-; dolerite /trachyte/tuff/basalts/volcanic, layer-5; and stringers of sandstone, shale and limestone that sits above the basement as layer-6. These rock formations (layers) are assigned with seismic velocities, which are derived from the first arrival travel times from the seismograms (Figure 4). Further, based on the drilled lithology and the hidden layers from the seismic studies, we have assigned low velocity layers to the Mesozoic sediments, that exist below the Deccan volcanic (traps), as well as Mesozoic volcanics (Figure 2). These inputs are used for modelling of crustal seismic structure.

The first arrival travel times are picked up from seismograms to calculate true and apparent velocities (Figure 4). The travel time data from the all the shot points, reveals presence of a thin sedimentary layer with velocity varying from 1.9 - 2.2 km/s. Since this velocity is measured from the direct arrival times, it represents the true velocity of the exposed Tertiary sediments. Similarly, the measured apparent velocities are assigned to the corresponding rock formation based on well log data. The first LVL (layer-3) is correlated with Mesozoic sandstone, which is exposed at the surface near Dhrangadhra region of Saurashtra. It is characterized by velocity 3.8 km/s (Chari, 1974; Uniyal, 1985; Prasad et al., 1985). DSS studies carried out earlier along Tikor-Wankaner-Mangrol profile, has also reported a velocity of 3.1 km/s for the exposed Mesozoic sandstone (NGRI, 1998). Based on these velocities and lithostratigraphic thicknesses (~ 300 m) as obtained from the borehole results, we assign a velocity 3.3 km/s to match the travel time data. Presence of such sediments are also reported from the Banni, Danduka, Lodhika (Dixit et al., 2000) and GK-29A-1 borewells (Figure 2). A similar LVL (layer-6) above the basement, is also being reported here for the first time, that was not reported in earlier studies (Pandey et al., 2009; Prasad et al., 2010; Prasad et al., 2013). Also during modelling, it was found necessary to introduce a low velocity layer to match the observed data

Data modelling

To derive 2-D velocity model, we have used raytracing technique developed by Zelt and Smith, (1992) and Zelt (1999), which uses efficient ray tracing equations (Zelt and Ellis, 1988*)*. In this approach, the model is defined as a sequence of layers separated by boundaries. In each layer, the upper boundary and lower boundary is defined by P-wave velocity. During ray tracing, the model is discretized into irregular trapezoidal cells with dipping interfaces, and velocity is linearly interpolated within each cell using the P-wave velocities at its four corner points. A smooth layer boundary simulation is used to avoid scattering and focusing of ray paths. Based on dominant frequency (20 Hz) of the data, we assign uncertainties of 100 ms for the first arrival travel times, as signal is not strong enough due to the absorption of energy from the volcanic rocks. The detailed methodology is given in Chandrakala et al. (2015, 2023).

The modelling have been carried out by preparing an initial 1-D velocity model that has been derived from all the shot point data. This model has been refined until there is satisfactory agreement between the observed and calculated travel times. The top layer, which is exposed at the surface gives the true velocity of the formation. We followed layer stripping method, where the interface between the first and second and the velocity of second layer, are calculated by inverting travel time data. Thereby, we have derived the shallow depth section till the basement. The ray diagrams and corresponding travel time matches are shown in Figure 5.

Similarly, for deriving deeper depth section, we utilize the reflection data. We have picked up prominent reflection phases from each shot points. Reflections from the Moho is limited to only a few shot points due to the small profile length. Shot gathers of the shot point SP 1 is shown in Figure 6, which indicates the quality of the signals. In this record section, one can notice the strong reflection phase which looks like a continuous scratch over the seismograms, which is observed in a time window around 4 – 6 s (reduced travel time) and at a distance of 30 to 55 km from the shot location, that represent the reflections from the Moho (Figure 6)

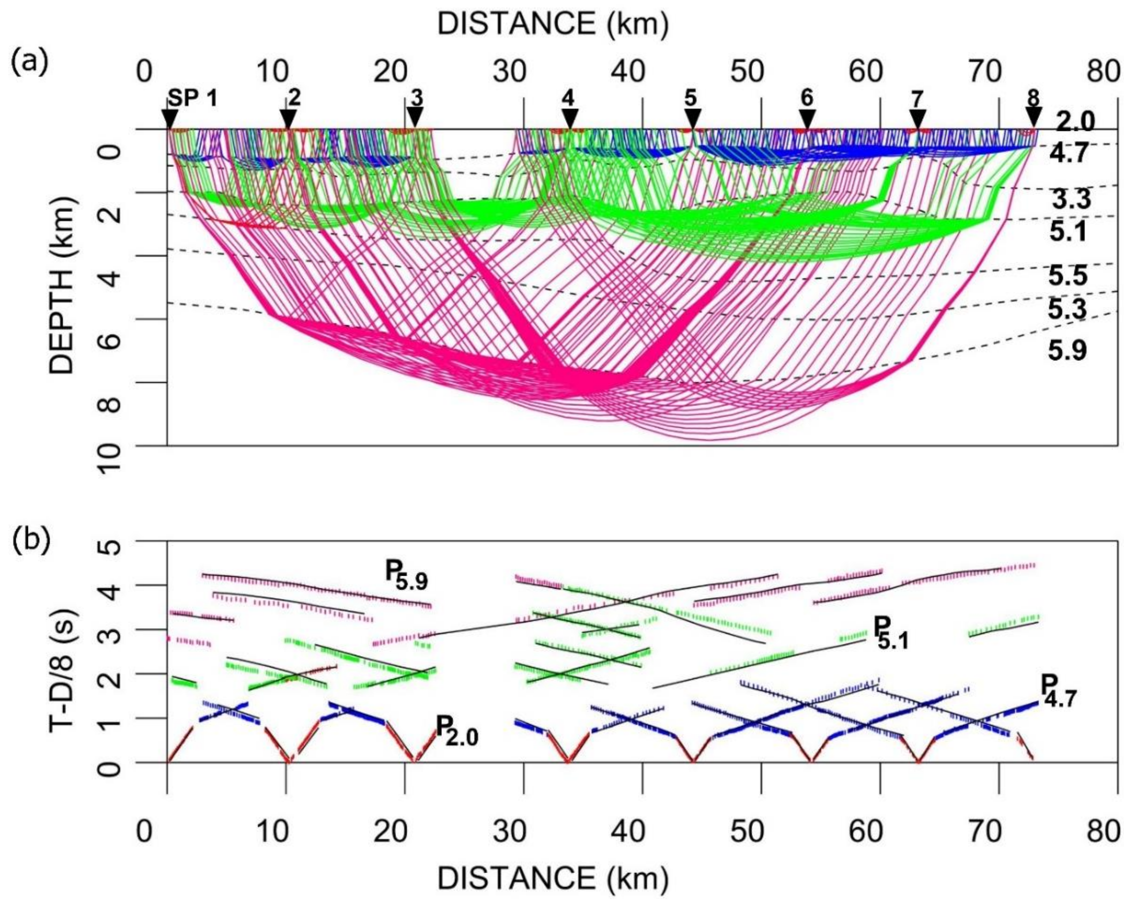

Figure 5. (a) Ray diagram showing the subsurface coverage by the refracted rays through the final derived velocity model. The numbers represent the velocity in km/s. **(b)** The comparison between the observed (vertical bars) and theoretical (solid lines) travel times for all the phases plotted in reduced travel time of velocity 8.0 km/s for clarity. The refraction travel time data is represented by various colours for various phases. Subscript represents refracted velocities.

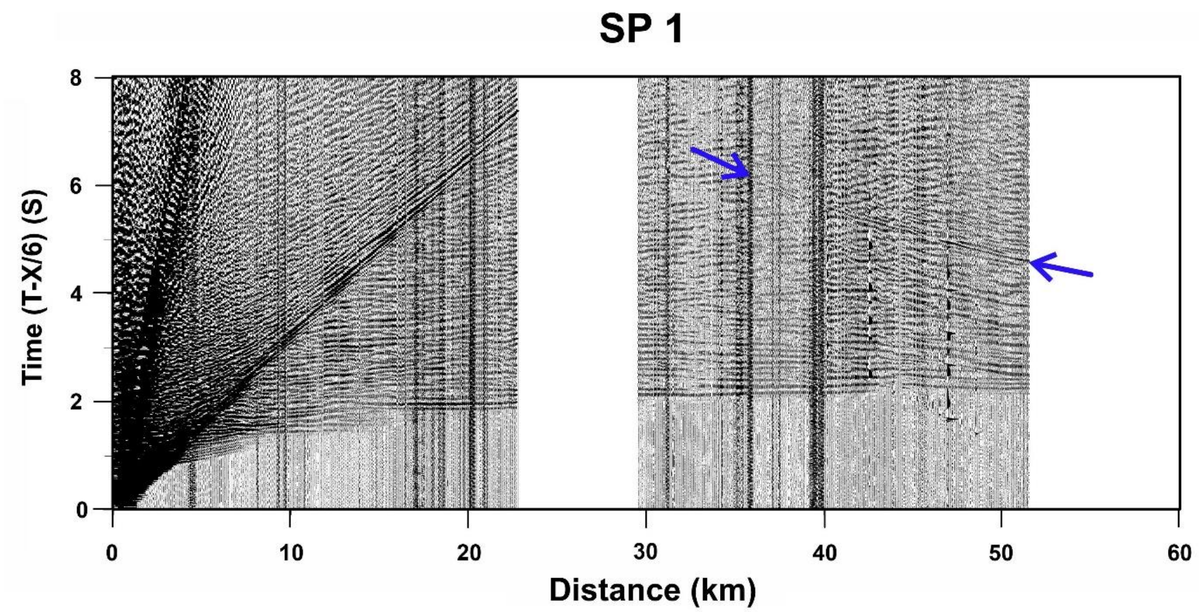

Figure. 6 Trace-normalized seismogram for shot point SP 1 shown with a reduction velocity of 6.0 km/s. Strong reflection phase from the Moho is indicated by blue arrow.

To improve the signal-to-noise ratio, we used the band pass filter (2-8-18-22 Hz) and isolated the signal from ground roll to enhance the quality of the data **(**Figure 7a). Once the reflections phases are identified, we have carried out modeling to match these reflection phases, as mentioned earlier. Due to the small profile length, the deeper section is prepared solely on the basis of reflection phases, as it lacks refractions from the deeper depths. The velocities for deeper depths have been considered from the nearby seismic studies *(*Kaila et al., 1980, 1990; Surya Prakasa Rao and Tewari 2005). The model has been modified until we obtained satisfactory agreement between the observed and calculated travel times for all the shot points.

The derived final model has been checked by comparing the relative amplitudes of observed phases to those with theoretical ones for each shot point by using ray theory code (Zelt and Smith, 1992). It can be seen from the record sections that there is a reasonably good agreement between the synthetic and the observed seismograms (Figure 7).

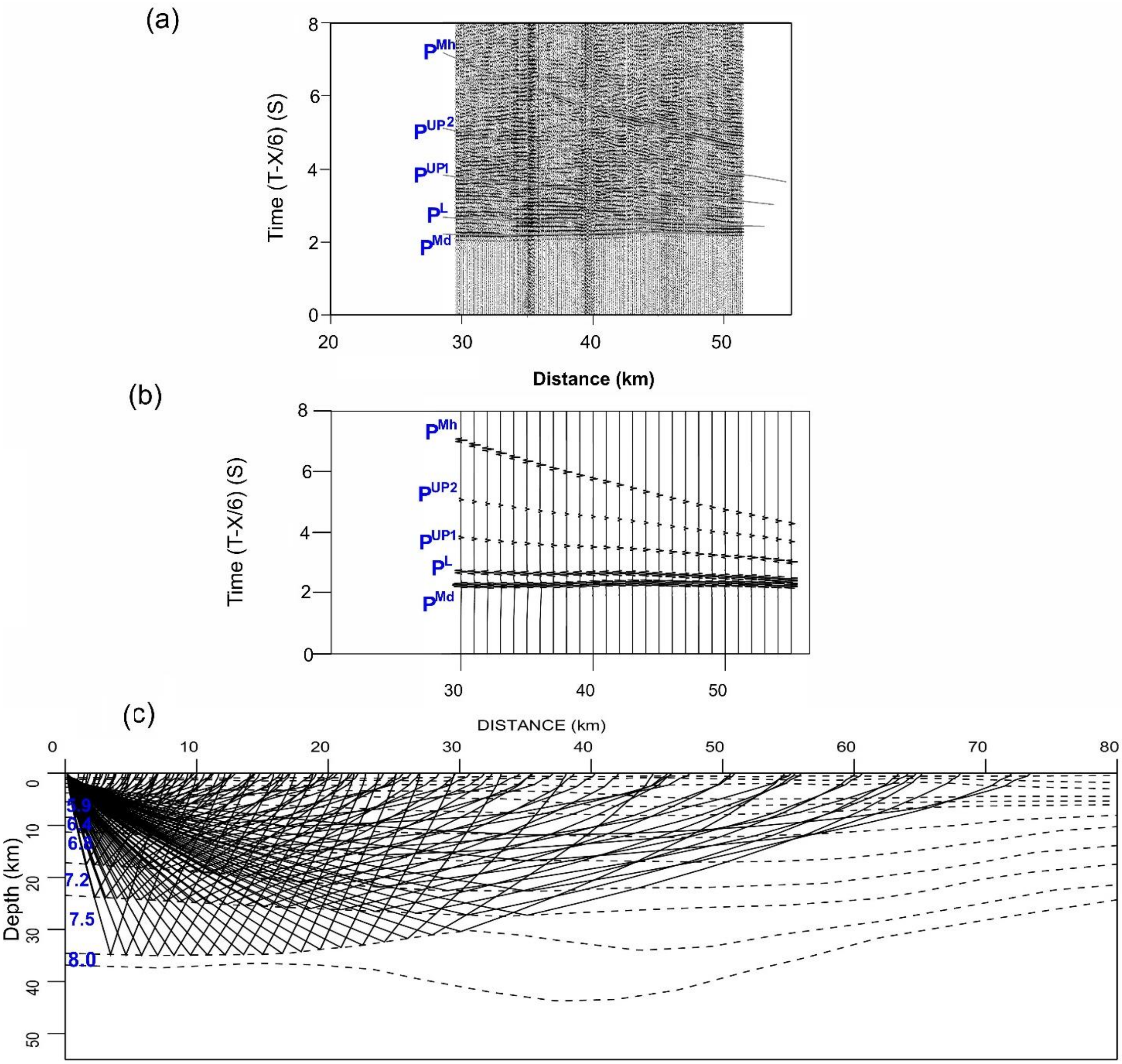

Figure 7. (a) Trace-normalized seismogram of shot point SP 1 with a reduction velocity of 6.0 km/s. Grey line represents theoretically calculated travel times through derived velocity model, which is overlapped on the seismogram to compare with the observed, and **(b)** the corresponding synthetic seismogram in the same distance range. **(c)** Ray diagram showing the subsurface coverage by reflected rays from various crustal layers. All distances marked on the X-axis are from 'zero' position of the model. Reflections from the top of the mid crust, lower crust, first and second underplated magmatic layers and the Moho, are represented by P^{Md} , P^{L} , P^{UP1} , $P^{UP2,}$ and P^{Mh} respectively. The numbers represent velocity in km/s.

The Moho usually produces a strong, coherent reflected phase in seismic records due to the significant change in acoustic impedance (density and velocity contrast). This reflection phase can be a sharp, discrete event or a band of reflectivity. In the present study, we have noticed sharp and coherent phases in shot points SP 1, SP 7 and SP 5 (Figures 6 and 8). We have further noticed that these strong reflection phases occur in a time window around 4 – 6 s (reduced travel time) and at a distance of 30 to 55 km from the shot location. Globally, such Moho reflection phases in the continental crust are usually observed around 10 - 14 s (two-way travel time), where as in the regions associated with crustal extension or rifting, the Moho can be located at around 7 to 9 s. Nevertheless in our case, the estimated two way time is around 4 – 6 s, that would indicate that the Moho is at much shallower depths.

Floating reflectors

While modeling the observed strong Moho reflection phases, we found it necessary to introduce floating reflectors, as it needed different Moho depths for the shot points SP1, 5 and 7. The reciprocity of the travel time and coherence of the signal indicated that these reflection phases are from the Moho boundary only (Figure 6, 8). In shot point SP 1, the theoretically generated reflections from the Moho are at a deeper depth of around 30-35 km and it matches well with the observed phase (Figure 7). Similarly, for SP 7, the Moho depth is relatively shallower than the SP 1, with different dip (Figure 8 b). But for SP 5, to match these Moho reflections, it requires relatively deeper depth. Due to limitations of this method, within the short distances, such reflections cannot be generated to match the observed data. Thus to match these reflection phases, we introduce floating structures using the algorithm from Zelt and Smith (1992) in order to constrain the geometry of these reflectors. Usually, such floating reflectors are introduced once velocities have been well resolved. Since, the floating reflecting boundaries are interfaces with no associated velocity discontinuity, it is called floating, where rays can reflect in addition to the layer boundaries. In the present study, we identify that these boundaries, occur below the Moho with continuation to shallow depths towards SP 1 (Figure 8a). In similar situations, floating reflectors has earlier been introduced by many workers worldwide (Epili and Mereu, 1991; Mooney and Meissner, 1992; Zelt and Forsyth, 1994; Zelt et al., 1994; Zelt and White, 1995; Luosto, 1997; Zelt,1999; Chandrakala et al., 2023). Location of the introduced floating reflectors and their corresponding match with the observed data, is included in Figure 8a b. In SP 7, theoretically generated reflections from the floating reflectors matches well with the observed phases (Figure 8 b). We show in Figures 9 and 10, the shallow and deep crustal velocity model as derived from the first arrival refraction and wide-angle reflection data and drilled borewell lithology.

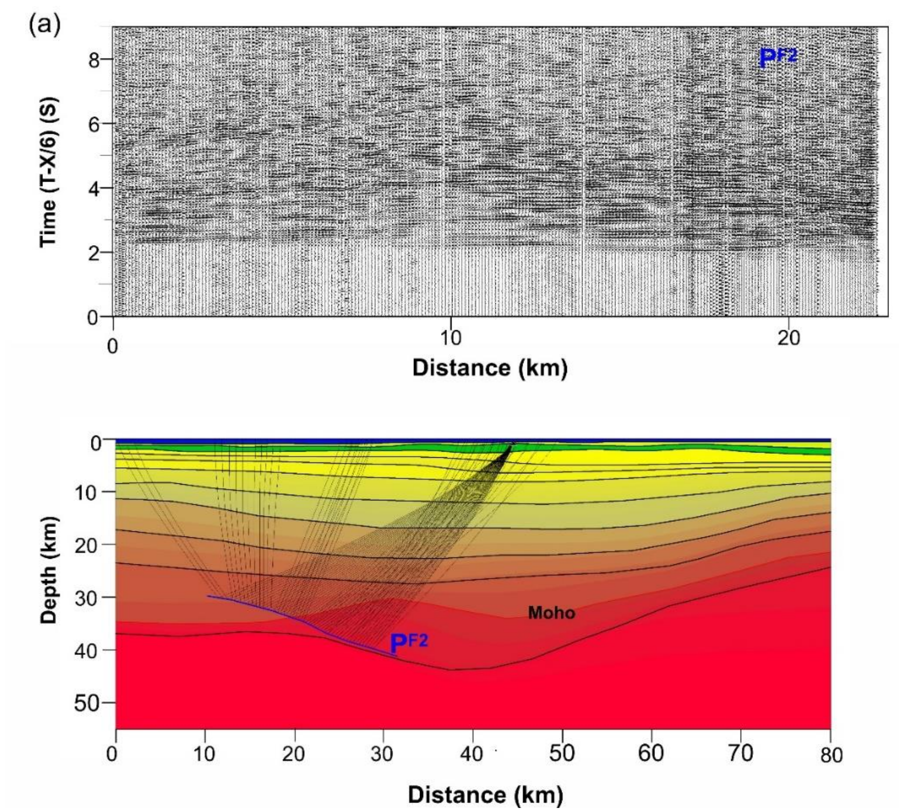

Continued…

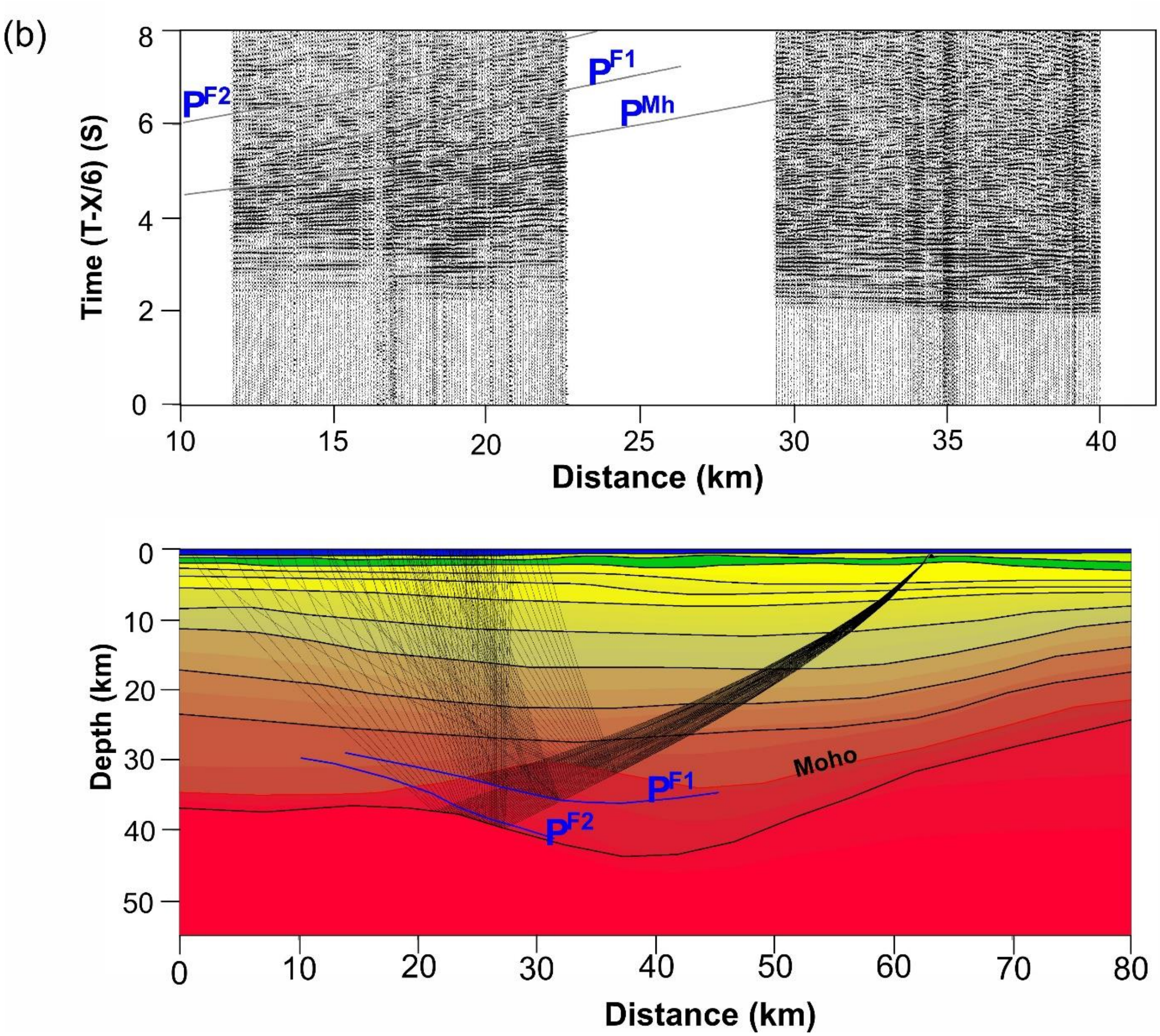

Figure 8. Trace-normalized seismogram of shot points **(a)** SP 5 and **(b)** SP 7, shown with a reduction velocity of 6.0 km/s. Theoretically calculated reflection phases from the Moho (P^{Mh}) and floating reflectors (P^{F1} and P^{F2}) are overlapped on the seismograms to show the match. All the distances marked on the x-axis are with reference to the zero position of the model.

RESULTS

Shallow crustal seismic structure

Figure 9 reveals presence of six distinct layers above the Precambrian granitic-gneissic basement, characterized by velocity 5.90 to 6.00 km/s. The first layer corresponds to exposed Tertiary sediments, exhibiting a very low average velocity of 2.0 km/s and has a thickness varying from 400 m to 900 m above the Deccan basaltic layer (Vp: 4.60-4.80 km/), which has a variable thickness. Deccan basalt is only about 300 m thick below Jakhau, compared to about 1400 m below the Mandvi, located at the eastern end of the profile, which is more than the maximum drilled thickness of about 1250 m in the Koyna seismic zone, located in the Western Ghats region (Mishra et al., 2017**)**. Below this layer, occurs a 1000 to 1300 m thick low velocity layer (LVL), with velocity 3.30 km/s, which corresponds to Mesozoic sandstone. It conforms with the drilled well information (Figure 2). It is underlain by relatively higher velocity Mesozoic limestone (Vp: 5.10 km/s) which overlie a thick (1000-2000 m) Mesozoic volcanic layer that has a considerably higher velocity of 5.50 km/s compared to Deccan volcanic layer (Vp: 4.7 km/s). It is further underlain by another Mesozoic sedimentary LVL layer, characterised by a velocity of 5.30 km/s. Its thickness varies from 1000 m to 2500 m. This layer directly rests over the Precambrian granitic-gneissic basement. We delineated two fault zones, located between SP 3 and SP 5, and SP 6 and 7. The first one may corresponds to Katrol Hill Fault.

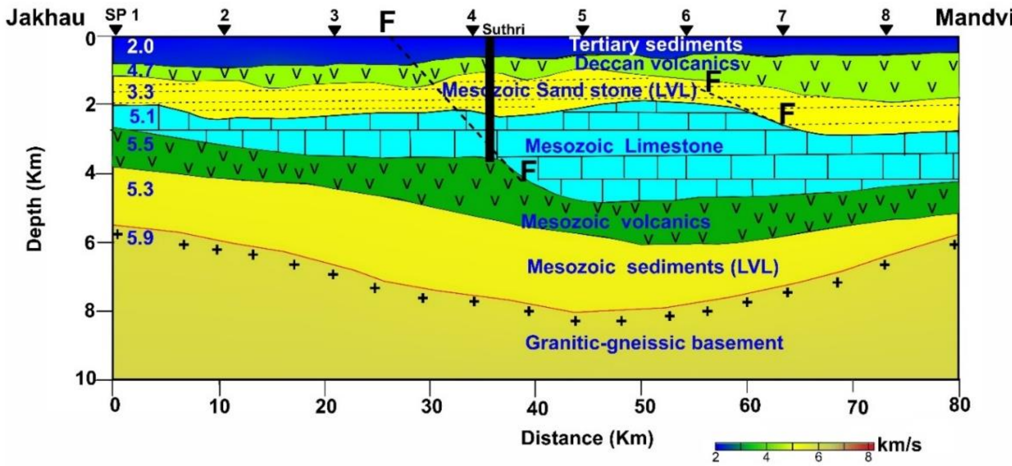

Figure 9. Shallow crustal seismic velocity section along the Jakhau – Mandvi seismic profile. Inverted triangle represents the shot point location. Red line represents the basement. Dash line indicates location of delineated faults (F). Velocities in different crustal layers are in km/s. Location of Suthri well, which falls in the closed vicinity of the profile, is also shown.

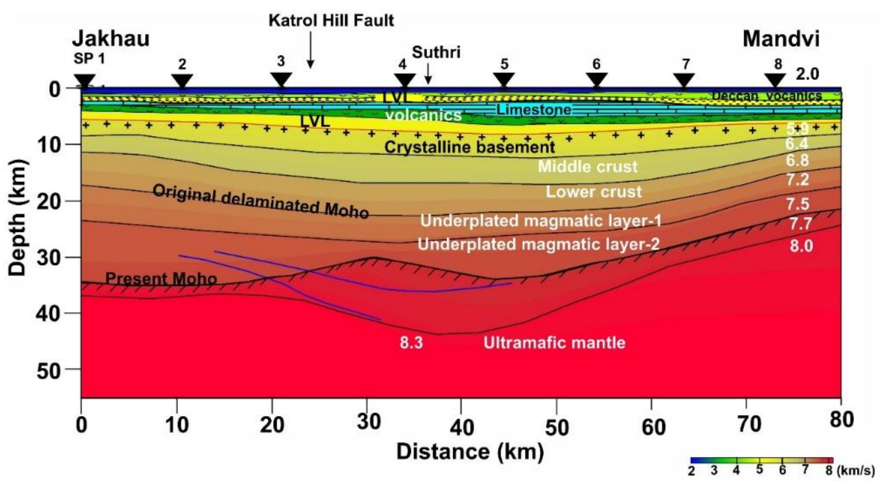

Figure 10. Final crustal seismic velocity depth section along Jakhau–Mandvi DSS profile. Inverted triangle represents the shot point location. The basement is shown by red line. Blue line indicates floating reflectors. Velocities in different crustal layers are in km/s.

Deeper crustal seismic structure

The deeper crustal section, as shown in Figure 10**,** indicates that the depth to the Precambrian granitic-gneissic basement (5.9-6.0 km/s) along the profile varies about 5.5 km to 8 km, maximum being observed between SP 4 and SP 6. It rests over a mid-crustal layer characterize by velocity of 6.30-6.40 km/s and its depth varies from 8 to 12.5 km from the surface. It is underlain by the mafic lower crust (Vp: 6.80-6.90 km/s) which has a much smaller thickness of 4.5 to 6.5 km only. The derived model further exhibits the occurrence of two distinct underplated magmatic layers, around 8 to 17 km thick. It is quite thick below Jakhau and relatively thinner below SP 3 to SP 5, which coincides with the Katrol Hill Fault. The top magmatic layer (UP1) is characterised by a velocity 7.20 km/s, while the bottom one (UP2), has a much higher velocity of 7.50 km/s. Such high velocities at the base of the crust would represent a zone of severe crust-mantle thermal interaction.

Further, the Moho is characterized by a velocity of 7.7 - 8.0 km/s. Moho is conspicuously shallow at the depth of 25 km near Mandvi (Vp: 7.7 km/s) compared to about 35 km near Jakhau (Vp: 8.0 km/s). There is a noticeable upwarping of the Moho to about 30 km below SP 4. Importantly, our study also delineated presence of a frozen mantle magma chamber (Vp: 8.0 km/s) below the Moho in the uppermost mantle, which occurs below SP 3 to SP5. Its bottom is bounded by the normal ultramafic mantle (8.3 km/s) at 43 km depth (Figure 10). It coincides with the location of Katrol Hill Fault. It may have been formed due to mantle upwelling caused by strong crust-mantle thermal interaction.

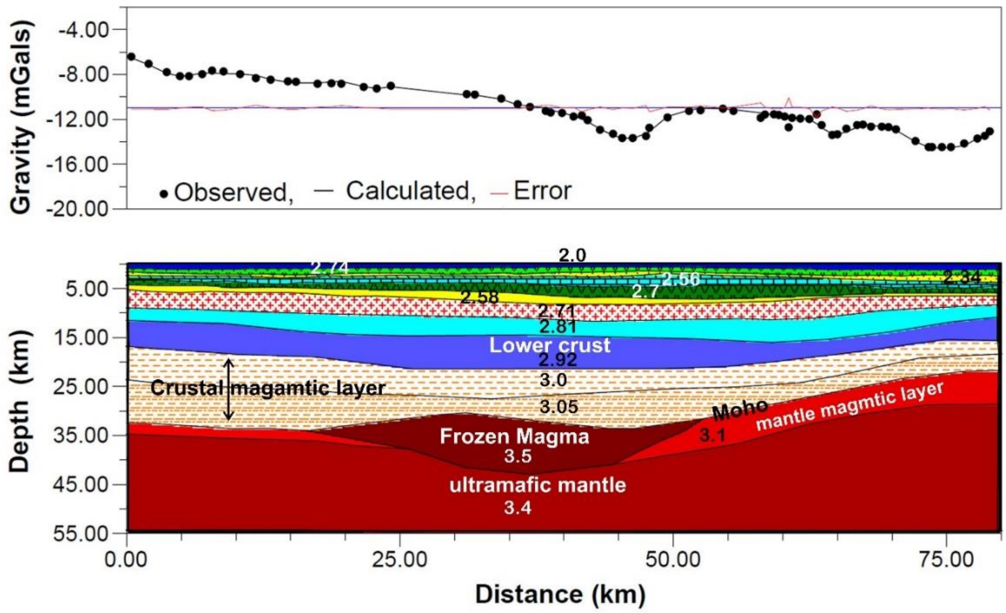

Figure 11. Comparison of observed and computed gravity response over the derived crustal density model, based on the seismic structure imaged along Jakhau –Mandvi DSS profile. The density values are in g/cm^3.

GRAVITY MODELLING

We also made an attempt to model the gravity field along the studied profile using the seismic constraints from the present study. Over this region, the gravity data was acquired with 5 mGal interval during 1997-1999. For the present study, we used the Bouguer gravity values along this profile from NGRI (2000) (Figure 11), which shows a large regional variation from NW to SE. To carry out two-dimensional gravity modelling, we use GM-SYS software (Geosoft Oasis Montaj, 2004). In this method, the response is calculated based on the algorithms of Talwani et al. (1959), Talwani and Heirtzler (1964) and Won and Bevis (1987). Following that, inversion calculations are made using algorithm of Marquardt (1963). The number of iterations (close to reality) with less RMS error provides the best-fit model. We converted derived crustal seismic structure into density using the velocity-density relationship of Nafe and Drake (1957) and Ludwig et al. (1970). The values of the input parameters and depth of the each layers have been accordingly changed to minimize the difference in a least square sense between the observed and computed Bouguer gravity fields. The derived gravity model is shown in Figure 11**,** which corroborates well with the obtained seismic image

DISCUSSIONS

Sediment thickness and crust-mantle structure

The shallow crustal section (Figure 9**)** revealed presence of six distinct layers above the granitic-gneissic basement (Vp: 5.90 to 6.00 km/s) with a maximum estimated thickness of 8 km. It is comprised of Tertiary sediments, Deccan basaltic layer, Mesozoic Limestone and two low velocity Mesozoic sedimentary layer (LVL). These Mesozoic sediments extend further into the Gulf of Kutch, where its reported thickness is between 2 and 4 km (Gopala Rao et al., 2021). Apart from this, sedimentary section also contains a 1 – 2 km thick Mesozoic volcanic layer, characterized by a relatively higher velocity (Vp: 5.5 km/s) than the overlying Deccan volcanics (Vp: 4.7 km/s). Its presence has been substantiated by the drilled-boreholes GK-29A-1 and Suthri (Figure 2), apart from Danduka and Lodhika wells in the Saurasthra region. In the Lodhika borehole, its drilled thickness is more than 500 m thick. This magmatic layer appears related to magmatism associated with Jurassic LIP (Large Igneous Province), which was formed during the India-Africa-Antarctica breakup (Leat, 2008). It may be thus surmised that even the Kutch and Saurashtra regions of western India, were severely affected by east Gondwana breakup, as also evidenced by the presence of subsurface Mesozoic volcanics and widespread thick magma underplating across the Moho (Figure 10). In this region, Moho is at extremely shallow depths due to subcrustal erosion and asthenospheric upwarp (Mandal and Pandey, 2010; 2011; Pandey, 2020). Magmatic extrusive activity during early Tertiary and Jurassic periods, is well reflected into regional uplifting and positive gravity anomalies over the Kutch and Saurashtra regions (NGRI 1998, 2000). Possibly, this region is still under going quaternary uplifting and substantial neotectonic activity, as indicated by recurring seismic activity. Being an ancient rift basin, it has been persistently active prior to and even during the Deccan volcanic episode (Biswas, 1987), as well as India –Eurasia collision. Currently, this region has been included in zone VI in the Earthquake hazard zone map (IS 1893, Part 1, 2025), which is comparable to Himalayan arc seismicity. This region is also strongly affected by the NE–SW compressive stress generated due to collision of Indian and Eurasian plates.

Anomalous shallowing of Moho

Consequent to the upwarping of the asthenosphere, the crust–mantle thermal interaction and subsequent sub crustal erosion, the Moho beneath this region is also seems to be severely affected. We found a conspicuously shallow Moho (only 25 km) near Mandvi, which has a quite lower Moho velocity (Vp: 7.7 km/s), compared to that found below the normal ultramafic mantle (Vp: > 8.0 km/s). Similarly, it is about 35 km deep near Jakhau. Recent studies based on multi-channel seismic reflection data and gravity modeling, Gopala Rao et al. (2021) derived a Moho thickness between 15 and 18 km in Gulf of Kutch region. Similarly, Chopra et al. (2014), analysed the crustal seismic structure of Gujarat through tele seismic receiver function studies. In their study, two of their seismic stations Naliya (NAL, 23.33°N, 68.83°E) and Gadhshisha (GDS, 23.10° N, 69.34°E) falls close to our seismic profile. It is interesting to see that they also found a shallow Moho thickness of 26.5 and 30.5 km respectively for these two stations. It appears that the Gulf of Kutch may be rifting and percolating to the main land of Gujarat due to persistent magmatism, massive sub crustal erosion and asthenospheric upwarping.

Massive magma underplating

A significant part of the lower crust worldwide is often seen stacked- up by the mantle-derived reworked magmatic rocks, consequent to the lower crustal and hot lithospheric mantle interaction (Rudnick and Fountain, 1995; Gao et al., 1998; Pandey et al., 2013; Pandey, 2020). Figure 10 indicates that the studied region too is underplated by an unprecedented thick layer of accreted magmatic rocks, just above the Moho. It is located at a depth between 15 and 23 km all along the profile. The crustal magmatic layer is about 8 to 17 km thick from place to place. It is characterised by two distinct velocities, 7.20 km/s in upper magmatic layer (UP1) and a much higher velocity 7.50 km/s in the lower magmatic layer (UP-2). Besides, we also found a lens-type mantle magmatic body at the base of the crust in the uppermost part of the mantle as well, which extends below SP 3 to SP 6. This region coincides with the Katrol Hill Fault. We attribute this body to a frozen magma chamber. This body is quite thick at about 12 to 13 km below SP 3 to SP 4. It has a high modelled density of 3.5 g/cm^3 representing contribution from the deeper hot mantle interaction.

Our findings are well supported by the detailed receiver functions studies carried out by Mandal and Pandey (2010, 2011). They used teleseismic events from 14 broadband seismic network, deployed over the Kutch seismic zone and obtained One-dimensional velocity model for the Vp and Vs derived from the three dimensional velocity tomograms below the 2001 Bhuj earthquake region. They reported 10 km thick underplated magmatic layer between the depth of 24 and 34 km above the Moho, which is further followed by 8 km thick differentiated Mantle magmatic layer between 34 and 42 km, characterized by velocity of 7.75-8.11 km/s which compares favourably with Vp: 8.0 km/s obtained for the mantle magma layer below SP3 to SP 6. Haldar et al. (2022) also carried out receiver functional studies in the Kutch and Saurashtra region and found the presence of mafic/ultramafic material in the crust-mantle transition zone. Below the central part of the Kutch region, estimated heat flow (61.3 mW/m^2), the Moho temperature (630° C) and Mantle heat flow (43 mW/m^2) are also quite high (Vedanti et al., 2011; Pandey et al., 2017). Consequently, below this region, the LAB is highly upwarped to a shallow depth of around 63 to 70 km only (Mandal and Pandey, 2011; Pandey et al., 2017; Pandey, 2020).

CONCLUSIONS

Reprocessing of the seismic data along Jakhau-Mandvi profile, reveals an extremely unusual crust-mantle structure underneath. It provided some significant results about the evolutionary nature of this seismically active region. The following major conclusions can be drawn from the present study:

1. The shallow crustal seismic section contains six-layered sequence (i) Tertiary sediments (1.9 - 2.2 km/s), (ii) Deccan basalts (4.70 km/s), (iii) low velocity Mesozoic sediments - I (3.30 km/s), (iv) Mesozoic limestone (5.1 km/s), (v) Mesozoic volcanic (5.50 km/s), and (vi) low velocity Mesozoic sediments-II (5.30 km/s) above the crystalline basement that occurs at the depths of about 5.5 km to 8 km. It is followed by a mid-crustal (Vp: 6.30-6.40 km/s) and a relatively thin lower crustal layer (Vp: 6.80-6.90 km/s).

2. We find presence of two distinct underplated magmatic layers associated with varying velocities (Vp: 7.20 -7.50 km/s), with their thickness ranging from 8 to 17 km, indicating a strong crust- mantle thermal interaction and massive subcrustal erosion due to mantle upwelling.

3. Moho is found to be at an extremely shallow depths of about 25 km near Mandvi, and 35 km near Jakhau.

4. Further, we also found a frozen mantle magma chamber (Vp: 8.0 km/s), which is located just below the Moho and coincides with the location of Katrol Hill Fault.

Acknowledgements

The permission accorded by the Director, CSIR- National Geophysical Research Institute, Hyderabad to publish this work is gratefully acknowledged. We sincerely thank Dr. O. P. Pandey, Chief Editor of the Journal of Geophysical Union (JIGU) and the two anonymous learned reviewers for their immensely helpful comments that greatly improved the quality of our paper. KC thanks the Department of Science and Technology (New Delhi) for the financial support to carry out this study through a project SR/WOS-A/EA-62/2021(G). We acknowledge Mrs. K. Renuka for her assistance in seismic data processing. We owe our sincere thanks to the DSS field persons for acquiring high quality seismic data.

Authors Contribution

K. Chandrakala: Data curation, methodology, seismic and gravity modelling, conceptualization, interpretation, original draft writing, Prakas Kumar: Guiding the research work, review and editing.

Data Availability

Basic data is available with CSIR- NGRI, Hyderabad.

Compliance with Ethical standards

No conflict of interest and authors adhere to copyright norms.

REFERENCES

Biswas, S.K., 1987. Regional framework, structure and evolution of the western marginal basins of India. Tectonophysics, 135, 302–327.

Biswas, S.K., 2005. Special section: Intraplate seismicity a review of structure and tectonics of Kutch basin , western India, with special reference to earthquakes. Curr. Sci., 88, 1592–1600.

Chandrakala, K., Pandey, O. P., Prasad, A. S. S. S. R. S. and Sain, K., 2015. Seismic imaging across the Eastern Ghats Belt-Cuddapah Basin collisional zone, southern Indian Shield and possible geodynamic implications. Precamb. Res., 271, 56–64.

Chandrakala, K., Pandey, O.P., Mandal, B and Prasad, A.S.S.S.R.S., 2023. Complex Crust-Mantle Seismic Structure below North Cuddapah Basin-Eastern Ghats Collisional Belt, South Indian Shield: Regional geodynamics and East Antarctica Correlation. J. Asian Earth Sci., 248, 105606. DOI: 10.1016/j.jseaes.2023.105606.

Chari, K.V., 1974. Refraction and seismic survey in Viramgam, Surendranagar, Wadhwan, Sayla, Chotila, Saurashtra, Gujarath, ONGC Rep (unplublished).

Chopra, S., Chang, T.M., Saikia, S., Yadav, R.B.S., Choudhury, P. and Roy, K.S., 2014. Crustal structure of the Gujarat region, India: New constraints from the analysis of teleseismic receiver functions. J. Asian Earth Sci., 96, 237-254. doi.org/10.1016/j.jseaes.2014.09.023.

Chung, W.Y. and Gao, H., 1995. Source parameters of the Anjar earthquake of July 21, 1956, India and its seismtectonic implications for the Kutch rift basin. Tectonophysics, 242, 281–292.

DGH, 2015. National Data Repository, Directorate General of Hydrocarbons(DGH), MoPNG, Government of India (https://www.ndrdgh.gov.in/NDR/?page_id=742)

Dixit, M. M., Vani, N. S., Sarkar, D., Khare, P. and Reddy, P. R., 2000. Velocity inversion in the Lodhika area, Saurashtra peninsula, Western India. First Break, 18, 499-504. doi.org/10.1046/j.1365-2397.2000.00109.x.

Dobrin, M. B. 1976. Introduction to geophysical prospecting (3rd ed.). McGraw-Hill.

Epili, D. and Mereu, R.F., 1991. The Grenville Front Tectonic Zone: Results from the 1986 Great Lakes onshore seismic wide-angle reflection and refraction experiment. J. Geophys. Res., 96, 16335–16348.

Gambos, A.M., Powell Jr. W.G. and Norton, I.O., 1995. The tectonic evolution of western India and its impact on hydrocarbon occurrences: an overview. Sediment. Geol., 96, 125–130.

Gao, G., Luo, T.C., Zhang, B.R., Zhang, H.F., Han, Y.W., Zhao, Z.D. and Hu, Y.K., 1998. Chemical composition of the continental crust as revealed by studies in east China. Geochim. Cosmochim Acta, 62, 1959-1975.

Gao, S.S., Kelly, H., Liu, H. and Chen, C., 2004. Significant crustal thinning beneath the Baikal rift zone: new constraints from receiver function analysis. Geophys. Res. Lett., 31, L20610:1–L20610:4.

Geosoft Oasis Montaj. 2004. GM-SYS version 7.0 Gravity and magnetic modeling software user guide. Northwest Geophysical Associates Inc.

Gopala Rao, D., Krishna, K.S., Harinarayana, T., Veeraswamy, K., Abdu Azeez, K. K., Ismaiel, M., Chaubey, A. K., and Srinivas, K.and Sreejith, K.M., 2021. Crustal structure of the Gulf of Kachchh, northwest India. J. Earth Syst. Sci., 130, 1-16.
doi.org/10.1007/s12040-021-01623-0.

Gupta, H. K., Harinarayana, T., Kousalya, M., Mishra, D.C., Indra Mohan, Puranachandra Rao, N., Raju, P.S., Rastogi, B.K., Reddy, P.R. and Sarkar, D., 2001. Bhuj earthquake of 26th January, 2001. J. Geol. Soc. India, 57, 275–278.

Haldar, C., Prakash Kumar, Pandey, O.P., Sain, K. and Kumar, S., 2022. Lower crustal intraplate seismicity in Kachchh region (Gujarat, India) triggered by crustal magmatic infusion: Evidence from shear wave velocity contrast across the Moho, Geosyst. Geoenviron., 1(3), doi.org/10.1016/j.geogeo.2022. 100073.

IS 1893, Part 1, 2025. Design earthquake hazard and criteria for earthquake-resistant design of structures-Code of practice Part 1: General provision (seventh revision).

Johnston, A.C., 1994. Seismotectonic interpretations and conclusions from the stable continental region seismicity data base, Chapter 4. In: The Earthquakes of stable continental regions , Vol. 1, Assessment of large earthquake potential, prepared by A.C. Johnston et al., prepared for Electric Power Research Institute, Calif. (USA), p.4-1 to 4-103.

Johnston, A.C., 1996. Seismic moment assessment of earthquakes in stable continental regions. Geophys. J. Int., 124, 381–414.

Kaila, K. L., Tewari, H. C. and Sarma, P. L. N., 1980. Crustal structure from deep seismic sounding studies along Navibandar-Amreli profile in Saurashtra, Mem. Geol. Soc. India, 3, 218–232.

Kaila, K. L., Tewari, H.C., Krishna, V.G., Dixit, M.M., Sarkar, D. and Reddy, M. S., 1990. Deep seismic sounding studies in the north Cambay and Sanchor basins, India, Geophys. J. Int., 103, 621–637

Kayal, J.R., Zhao, D., Mishra, O.P., De, R. and Singh, O.P., 2002. The 2001 Bhuj earthquake: tomographic evidence for fluids at the hypocenter and its implications for rupture nucleation. Geophys. Res Lett., 29, 2152–2155.

Kolluru, R. and Behera, L. (2025). Imaging intra-volcanic Mesozoic sediments and shallow crustal configuration from traveltime inversion of long-offset seismic data in

Saurashtra basin, India. J. Ind. Geophys. Union, 29(4), 218-235.

Koteswara Rao, P., Dixit, M.M., Khare, P., Kesava Rao, G., Raju, S., Sain, K., Murthy, A.S.N., Sarma, V.Y.N., Prasad, ASSSRS, Sridher, V., Reddy, M.S., Reddy, P. R. and Sarkar, D., 2004. Hidden Mesozoic Sediments – Searching with Seismic Refraction Tool. 5th Conference & Exposition on Petroleum Geophysics, pp 81-84.

Kruger, F., Scherbaum, F., Rosa, J.W.C., Kind, R., Zetsche, F. and Hohne, J., 2002. Crustal and upper mantle structure in the Amazon region., Brazil. determined with broadband mobile stations. J. Geophys. Res., 107 (B10) ESE 17-1–17-12.

Leat, P.T., 2008. Ferrar Large Igneous Province, Antarctica. In: The Geol. Soc. London, Special Publ., 302, 45–66.

Liu, L. and Zoback, M.D., 1997. Lithospheric strength and intraplate seismicity in the New Madrid seismic zone. Tectonics, 16, 585–595 .

Ludwig, W. J., Nafe, J. E. and Drake, C. L., 1970. Seismic refraction. In A. E. Maxwell (Ed.), The Sea (pp. 53–84). New York: Wiley-Interscience.

Luosto, U., 1997. Structure of the Earth's Crust in Fennoscandia as Revealed from Refraction and Wide-Angle Reflection Studies. Geophysica, 33, 3–16.

Lutter, W.J., Catchings, R.D. and Jarchow, C.M., 1994. An image of the Columbia Plateau from inversion of high-resolution seismic data. Geophysics, 59, 1278–1289.

Mandal, P., 2006. Sedimentary and crustal structure beneath Kachchh and Saurashtra regions, Gujarat, India. Phys. Earth Planet. Int., 155(3–4), 286–299.

Mandal, P., 2007. Sediment Thicknesses and Qs vs. Qp relations in the Kachchh rift basin, Gujarat, India using Sp converted phases. Pure Appl. Geophys., 164, 135–160.

Mandal, P. and Pujol, J., 2006. Seismic imaging of the aftershock zone of the 2001 Mw 7.7 Bhuj earthquake, India. Geophys. Res Lett., 33. doi: 10.1029/2005GL025275 .

Mandal, P. and Chadha, R.K., 2008. Three-dimensional velocity imaging of the Kachchh seismic zone, Gujarat, India. Tectonophysics, 452, 1–16.

Mandal, P. and Pandey, O.P., 2010. Relocation of aftershocks of the 2001 Bhuj earthquake: a new insight into seismotectonics of the Kachchh seismic zone, Gujarat, India. J. Geodyn., 49, 254–260.

Mandal, P. and Pandey, O. P., 2011. Seismogenesis of the lower crustal intraplate earthquakes occurring in Kachchh, Gujarat, India. J. Asian Earth Sci., 42, 479–491.

Marquardt, D. W., 1963. An algorithm for least squares estimation of non-linear parameters. J. Soc. Industrial Appl. Math., 11, 431–441.

Merh, S.S., 1995. Geology of Gujarat. Geological Society of India, 170pp.

Mishra, S., Vyas, D., Nikalje, D., Warhade, A. and Roy, S., 2017. A 1251m-thick Deccan flood basalt pile recovered by scientific drilling in the Koyna region, western India. J. Geol. Soc. India, 90, 788–794.

Mooney, W. D. and Meissner, R., 1992. Multi-genetic origin of crustal reflectivity: a review of seismic reflection profiling of the continental lower crust and MOHO, In: Fountain, D. M., Arculuta, R., Kay.(Eds) Continental lower crust, Elsevier Sci., 45-79.

Mooney, W.D., Andrews, M.C., Ginzburg, A., Peters, D.A. and Hamilton, R.M., 1983. Crustal structure of the northern Mississippi embayment and a comparison with other continental rift zones. Tectonophysics 94, 327–348.

Mukherjee, S.M., 1942. Seismological features of the Satpura earthquake of the 14th March 1938. Pro. Indian Acad. Sci., 16, 167–175.

Nafe, J.E. and Drake, C.L., 1957. Variation with depth in shallow and deep water marine sediments of porosity, density and the velocities of compressional and shear waves. Geophysics, 22, 523-552.

NGRI, 1998. Integrated geophysical studies for Hydrocarbon exploration Saurashtra, India. NGRI Technical report No. NGRI-98-EXP-237.

NGRI, 2000. Integrated Geophysical Studies for Hydrocarbon Exploration, Kutch, India. Technical Report: NGRI 2000-EXP-296. pp. 1–195.

Pandey, D., Singh, S., Sinha, M. and MacGregor, L., 2009. Structural imaging of Mesozoic sediments of Kachchh, India, and their hydrocarbon prospect. Marine Petrol. Geol., 26, 1043–1050.

Pandey, O. P., 2020. Geodynamic Evolution of the Indian shield: Geophysical Aspects. Springer Nature, Switzerland, 349pp .

Pandey, O.P., Vedanti, N., Srivastava, R.P. and Uma, V., 2013. Was Archean Dharwar Craton ever stable? A seismic perspective. J. Geol. Soc. India, 81, 774–780.

Pandey, O. P., Vedanti, N. and Srivastava, R, P., 2017. Complexity in Elucidating Crustal Thermal Regime in Geodynamically Affected Areas: A Case Study from the Deccan Large Igneous Province (Western India). J. Geol. Soc. India, 90 (3), 289–300.

Paul, J., Burgmann, R., Gaur, V.K., Bilham, R., Larson, K.M., Ananda, M.B., Jade, S., Mukal, M., Anupama, T.S., Satyal, G. and Kumar, G., 2001. The motion and active deformation of India. Geophys. Res. Lett., 28, 647-650.

Prasad, A.S.S.S.R.S., Sain, K. and Sen, M.K., 2013. Imaging sub basalt Mesozoics along Jakhau-Mandvi and Mandvi-Mundra profiles in Kutch sedimentary Basin from seismic and gravity modeling. Geohorizons, 51-55.

Prasad, B. R, Venkateswarlu, N., Prasad, A. S. S. S. R. S., Murthy, A. S. N. and Sateesh, T., 2010. Basement configuration of on-land Kutch basin from seismic refraction studies and modeling of first arrival travel time skips. J. Asian Earth Sci., 39(5), 460–469.

Prasad, S., Bapat, R.D. and Singh, R.B., 1985. Evolving a methodology for exploration of subtrappean Mesozoic sediments in Saurashtra-Phase-III . Acquistion, Processing and interpretation of data of Refraction Lines 2-1-1R and 201-2R of field season 1983-1984, ONGC Rep (unpublished).

Prodehl, C., Keller, G.R. and Khan, M.A., 1994. Crustal and upper mantle structure of the Kenya rift. Tectonophysics, 236, 1–483.

Rajendran, C.P. and Rajendran, K., 2001. Characteristics of deformation and past seismicity associated with the 1819 Kutch Earthquake, Northwestern India. Bull. Seismol. Soc. Am., 91 (3), 407–426.

Rajendran, C.P., Rajendran, K., Thakkar, M. and Goyal, B., 2008. Assessing the previous activity at the source zone of the 2001 Bhuj earthquake based on the near- source and distant paleoseismological indicators. J. Geophys. Res., 113 B05311, doi:10.1029/20 06JB0 04845.

Rogers, J.J.W. and Callahan, E.J. 1987. Radioactivity, heat flow and rifting of the Indian continental crust. J. Geol., 95, 829–836.

Rudnick, R.L. and Fountain, D.M., 1995. Nature and composition of the continental crust: a lower crustal perspective. Rev. Geophys., 33, 267–309.

Sarkar, D., Sain, K., Reddy, P.R., Catchings, R.D., Mooney, W.D., Stein, S. and Mazzotti, S., 2007. Seismic-reflection images of the crust beneath the 2001M = 7.7 Kutch (Bhuj) epicentral region, western India. In: Continental Intraplate Earthquakes: Science, Hazard, and Policy Issues. Geol. Soc. America, 425, 319–327 .

Singh, D., Alat, C.A., Singh, R.N. and Gupta, V.P., 1997. Source rock characteristics and hydrocarbon generating potential of Mesozoic sediments in Lodhika Area, Saurashtra Basin, Gujarat, India. Proceedings Second Int. Pet. Conference & Exbn. Petrotech-1997, New Delhi, India, pp 205-220.

Singh, S.K., Dattatrayam, R.S., Shapiro, N.M., Mandal, P., Pacheco, J.F. and Midha, R.K., 1999. Crustal and upper mantle structure of Peninsular India and source parameters of the May 21, 1997, Jabalpur earthquake., Mw = 5.8.: results from a new regional broadband network. Bull. Seismol. Soc. Am., 89, 1632–1641.

Surya Prakasa Rao, G. and Tewari, H. C., 2005. The seismic structure of the Saurashtra crust in northwest India and its relationship with the Réunion Plume, Geophys. J. Int., 160, 18–330.

Talwani, M. and Heirtzler, J. R., 1964. Computation of magnetic anomalies caused by two dimensional bodies of arbitrary shape. In G. A. Parks (Ed.), Computers in the mineral industries, Part 1. Stanford University Publication, Geological sciences, 9, 464–480.

Talwani, P. and Gangopadhyay, A., 2001. Tectonic framework of the Kachchh earthquake of 26 January 2001. Seism. Res. Lett., 72(3), 336–345.

Talwani, M., Worzel, J. L. and Landisman, M., 1959. Rapid gravity computations for two dimensional bodies with application to the Mendocino submarine fracture zone. J. Geophys. Res., 64, 49–59.

Tewari, H. C., Dixit, M. M. and Murty, R. K.,1995. Use of traveltime skips in refraction analysis to delineate velocity inversion1. Geophys. Prospect., 43(6), 793-804.

Uniyal, S.D., 1985. Operational report on refraction survey in Amreli-Kodinar area of Saurashtra, Gujarat state, ONGC Report. (unbpublished)

Vedanti, N., Pandey, O.P., Srivastava, R.P., Mandal, P., Kumar, S. and Dimri, V.P., 2011 Predicting heat flow in the 2001 Bhuj earthquake (Mw=7.7) region of Kachchh (western India), using an inverse recurrence method. Nonlin. Process. Geophys., 18, 611-625.

Whiteley, R.J. and Greenhalagh, S.A., 1979. Velocity inversion and shallow seismic refraction method. Geoexploration, 17, 125-141.

Wilson, D., Aster, R. The RISTRA Team, 2003. Imaging crust and upper mantle seismic structure in the southwestern United States using teleseismic receiver functions. Lead. Edge, 22, 232–237 .

Won, I. J. and Bevis, M., 1987. Computing the gravitational and magnetic anomalies due to a polygon: Algorithms and Fortran subroutines. Geophysics, 52, 232–238.

Zelt, C. A., 1999. Modeling strategies and model assessment for wide-angle seismic travel time data. Geophys. J. Int., 139, 183–204.

Zelt, C. A. and Ellis, R. M., 1988. Practical and efficient ray tracing in two dimensional media for rapid travel time and amplitude forward modeling. Canadian J. Expl. Geophys., 24, 16–31.

Zelt, C. A. and Smith, R. B., 1992. Seismic travel time inversion for 2-D crustal velocity structure. Geophys. J.Int.,108, 16–34.

Zelt, C.A. and Forsyth, D.A., 1994. Modeling wide-angle seismic data for crustal structure: Southern Grenville province. J. Geophys. Res. 99 (B6), 11687–11704.

Zelt, C.A. and White, D.J., 1995. Crustal structure and tectonics of the southeastern Canadian Cordillera. J. Geophy. Res. Solid Earth, 100 (B12), 24255–24273.

Zelt, C.A., Forsyth, D.A., Milkereit, B., White, D.J., Asudeh, I., and Easton, R.M., 1994. Seismic structure of the Central Metasedimentary Belt, southern Grenville Province. Can. J. Earth Sci., 31, 243–254.

Received on: 17-12-2025; Revised on 24-12-2025; Accepted on 24-12-2025